Using SG arrays for hydrology in comparison with GRACE satellite data, with extension to seismic and volcanic hazards

David Crossley
Department of Earth and Atmospheric Sciences, Saint Louis University; 3507 Laclede Avenue, St, Louis, MO 63103 USA, crossley@eas.slu.edu

Jacques Hinderer
Ecole et Observatoire des Sciences de la Terre, Institut de Physique du Globe de Strasbourg (UMR 7516 CNRS-ULP), 5 Rue Descartes, Strasbourg 67084 Cedex, France,

Abstract: We first review some history of the Global Geodynamics Project (GGP), particularly in the progress of ground-satellite gravity comparisons. The GGP Satellite Project has involved the measurement of ground-based superconducting gravimeters (SGs) in Europe for several years and we make quantitative comparisons with the latest satellite GRACE data and hydrological models. The primary goal is to recover information about seasonal hydrology cycles, and we find a good correlation at the microgal level between the data and modeling. One interesting feature of the data is low soil moisture resulting from the European heat wave in 2003. An issue with the ground-based stations is the possibility of mass variations in the soil above a station, and particularly for underground stations these have to be modeled precisely. Based on this work with a regional array, we estimate the effectiveness of future SG arrays to measure co-seismic deformation and silent-slip events. Finally we consider gravity surveys in volcanic areas, and predict the accuracy in modeling subsurface density variations over time periods from months to years.

Keywords: Superconducting gravimeter, GRACE, hydrology, ground truth, silent earthquakes, volcanic deformation

1. Introduction

We here discuss the potential of high quality gravimetric arrays to resolve problems of environmental and hazard interest. Our primary focus is on the use of superconducting gravimeters (SGs) because they offer the best combination of high precision and calibration stability but other gravimeters have been used in many situations where an SG installation has not been possible. Table 1 gives the most important parameters of 3 types of instrument. The values

Table 1 Comparison of Gravity Instruments.
(1 μGal = 10^{-9} g)

	Absolute Gravimeter AG (Transportable type, e.g. Micro-g Solutions Inc. FG5)	Relative Superconducting Gravimeter (Observatory and Transportable type: GWR)	Relative Spring Gravimeter (Field type: Scintrex CG-3M)
Precision	1 μGal	0.0001 μGal	3 μGal
Accuracy	1-3 μGal	0.1 μGal	3−10 μGal
Drift	0 (by definition)	1-5 μGal / yr	~ 400 μGal / day
Stabilization Time	1 hr (setup only)	days to weeks or longer	10 min (setup only)
Operation	Usually 1-3 days of continuous operation per measurement location, maximum period 2 weeks	Continuous unlimited measurement, with 2 x per year AG monitoring and calibration	Continuous unlimited measurement, with repeated ties every few hours to a reference site
Accuracy limited by	microseismic noise	environmental effects	instrument drift, elevation, environmental effects, calibration changes

have been taken from surveys reported in the literature, they are not necessarily the manufacturer's specifications. LaCoste & Romberg D meters have similar characteristics to the Scintrex, with slightly higher accuracy and lower drift.

Note that of the 3 types, the SG is the only one whose precision is 2-3 orders of magnitude better than the phenomena we are concerned with here (the 1 μGal level). Two other differences between the SG and the Scintrex are also important: the SG requires a relatively long conditioning period at each station for drift stabilization, whereas the Scintrex requires only a minimal time to set up. Second, the Scintrex calibration appears to be unstable and a local calibration line is recommended (Budetta and Carbone, 1997). By comparison the SG amplitude calibration is usually known to 1 part in 10^{-4} and is stable over periods of years (see e.g. Merriam, 1993). Figure 1 shows the raw output of the dual sphere SG (CD029, Table 4). Note that the upper sphere stabilizes almost immediately, but the lower one takes almost 200 days to reach its low drift. The drift curve is, however, very well defined and mathematically easy to model in the data, unlike the erratic drift of a spring instrument. Drift for SGs can either be exponential, as for CD029_L, or linear with time, and there is no predictable behavior one can use for all instruments. In several recent installations, the drift has stabilized over a month or so. Also in this figure, one can see a number of offsets that are different for each sphere; again these are generally possible to correct for, especially with the dual sphere instrument.

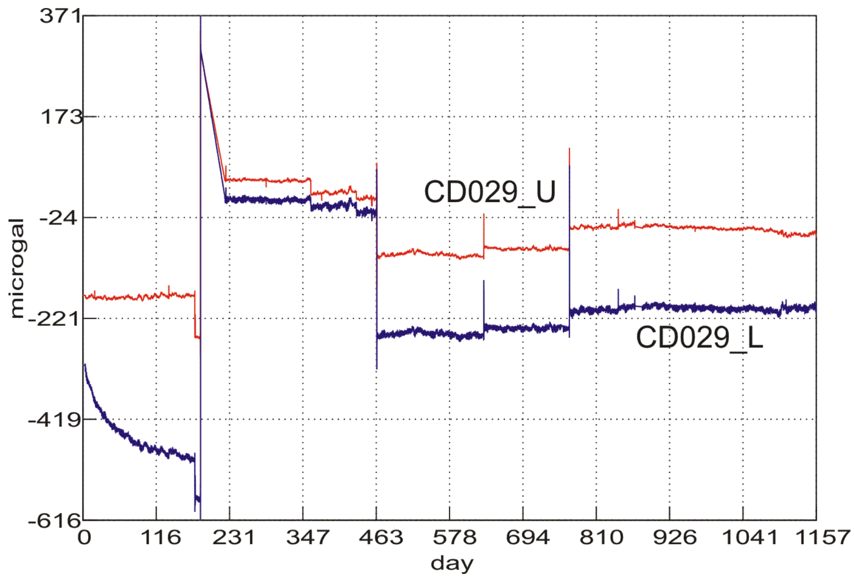

Figure 1 Initial raw data from the SG installed at Wettzell, Germany in November 1998. The two spheres (Upper, Lower) are separated vertically by several cm, and each responds differently to its magnetic environment, which is one of the causes of drift.

Signals of interest in gravity observations can be divided into two classes, depending on whether they are periodic or not. A review of recent investigations of both types of observations made with SGs of the Global Geodynamics Project (Crossley et al., 1999) can be found in Hinderer & Crossley (2004). Table 2 gives the gravity effects of harmonic components that have been studied by gravimeters.

Table 2 Periodic Signals – AMPLITUDE SPECTRUM
(Signal to noise ratio improves with length of record).

Cause	Amplitude (μGal)	Period Range
Earthquakes - Surface Waves	< 1000	10 - 100 s
Solid Earth Tides	0.001 - 300	6, 8, 12 hr etc.
Tidal Ocean Loading	< 10	… same …
Polar Motion, Annual / Chandler	1-10	1 yr, 435 day
Seismic Normal Modes	0.001- 0.1	5 s - 54 min
Slichter Triplet	~ 0.001	4 - 9 hr
Core Modes	< 0.001	12 – 24 hr

It can be seen that some of the signals have amplitudes of the order of 1 nanogal and these can only be seen under observatory conditions (i.e. with SG or possibly spring gravimeters) with relatively long records. Of more interest to this paper are the aperiodic signals associated with environmental effects or tectonic deformation of various kinds; these are listed in Table 3. Note that many of the signals are only a few μGal in amplitude and therefore at the limit of resolution of an AG or spring type gravimeter.

As seen in Table 1, the accuracy of the SGs has been demonstrated to be about 0.1 μGal. Klopping et al. (1995) gave one of the early demonstrations of this where two different types of SG were compared side by side over a period of several months. One was the UCSD type of gravimeter built by Goodkind, a research instrument, and the other was a commercial GWR compact model. Although these instruments had a common origin in the 1970's, by the 1990's they had become quite different. Nevertheless the time differences of the two residual signals were clearly less that 1 μGal.

A different example comes from the Moxa dual sphere instrument (Kroner et al., 2001), where both spheres are within the same dewar, but suspended by different coil systems. The data (Fig. 2) shows residual gravity from both spheres, with the sum and difference signals displayed. The difference signal remains mostly at or below 0.1 μGal, indicating this is the inherent accuracy of the instrument. Note the occasional (rare) offset between spheres over a period of 2 yr.

We conclude the introduction by providing Table 4 showing the admittances between gravity and station height, atmospheric pressure, and hydrology that are used at various points later on.

Table 3. Aperiodic Signals - POWER SPECTRAL DENSITY (Signal to noise ratio is independent of record length).

Cause	Amplitude (μGal)	Time Scales
Atmospheric Pressure Loading	< 5	min - yr
Non-Tidal Ocean Loading	~ 1	min - yr
Ocean Waves (microseisms)	< 10	1 - 12 s
Hydrology	< 20	min - yr
Co-Seismic / Silent Slip	1 - 3	hr - month
Volcanic Mass Motions	1 - 100	day - yr
Tectonics	~ 1	> 1 yr

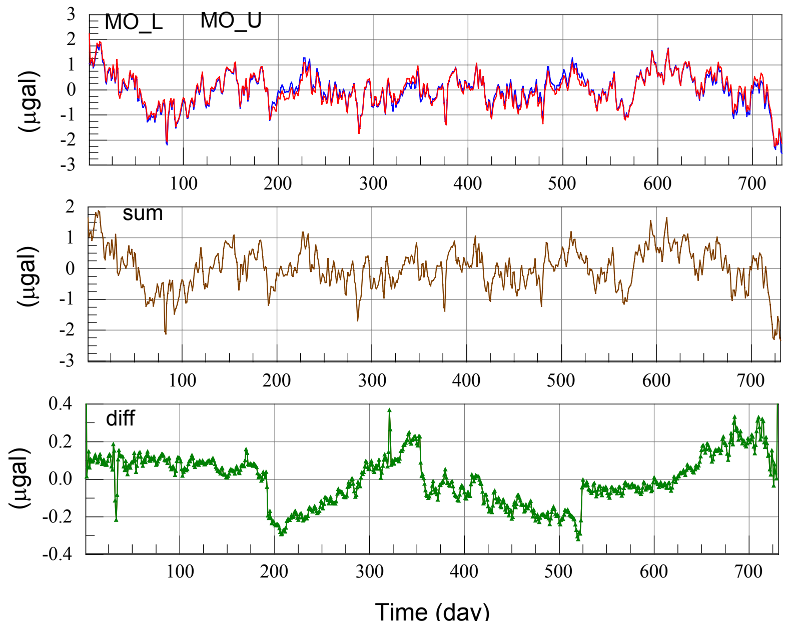

Figure 2. Residual gravity in μGal for the dual sphere SG in Moxa, Germany, installed in 1999. The upper curve shows the 2 data streams (blue upper trace, red lower trace) from Jan 1, 2000 over a 2-year period, and below is their sum (signal) and difference (noise).

Table 4. Useful Quantities

Surface Gravity	g	~ 9.8156 m s^{-2} ~ 10 m s^{-2}
	Δg	1 μGal (microgal) = 10^{-8} m s^{-2} ~ 10^{-9} g
		1 nGal (nanogal) = 0.001 μGal = 10 nm s^{-2}
(height effect)	admittance	Δg/Δh = - 0.31 μGal mm^{-1} (free air gradient, FA)
		Δg/Δh = - 0.2 μGal mm^{-1} (Bouguer corrected FA, or BCFA)
Atmospheric Pressure	p	1.01325 bar ~ 1 bar (at mean sea level)
	Δp	1 mbar = 0.001 bar = 1 hPa ~ 10^{-3} p
(pressure effect)	admittance	Δg/Δp = - 0.3 μGal mb^{-1}
Hydrology		
(layer thickness t)	admittance	Δg/Δt = 0.42 μGal cm^{-1} (infinite slab, 100% porosity)

2. GRACE – SG Comparisons

We report here briefly on two studies that have been done on the comparison of the continental size SG European array with hydrology and GRACE. The first study concerns a 4-year comparison of the SG gravity field with the predictions of global soil-moisture hydrology models driven by atmospheric inputs. A more detailed treatment is given in Crossley et al. (2004). The second will be a 2-year comparison of the SG data and hydrology with the time-varying gravity fields derived from GRACE.

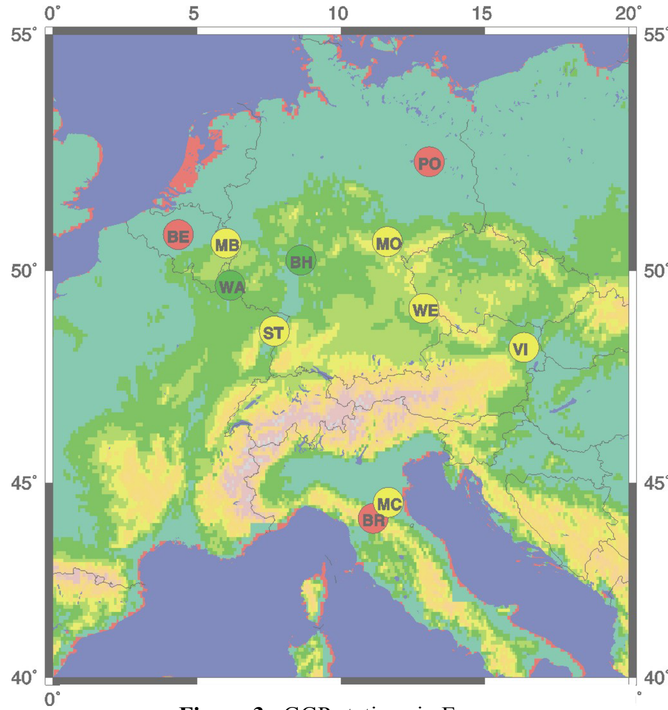

Figure 3. GGP stations in Europe.

2.1 Four Year Study Without GRACE Data

In the first study we used the 8 stations shown in Fig. 3. Stations in red are no longer operational, stations in yellow have mostly been recording since 1997 (except for MO which started in 1999) and stations in green are newer stations for which we do not have access yet to the data.

The purpose in using these stations is to generate a ground map of the varying gravity field with which to compare with the GRACE data. Individual SG stations are of course point measurements whereas GRACE sees only the longer wavelengths, perhaps down to about 500 km (nominal). In order for the SGs to be useful as ground truth for GRACE we have to demonstrate that the SG data can be averaged over continent sized areas, and that local effects at the stations do not overwhelm the longer wavelength information.

Fig. 4 shows the residual gravity series at each of the stations, all plotted to the same scale. Note there is a trace for station Metsahovi (ME) that is not included in the current discussion. Clearly such a plot does not give a clear spatial indication of the data variability, so we need to make a spatial average that can be compared to the satellite data.

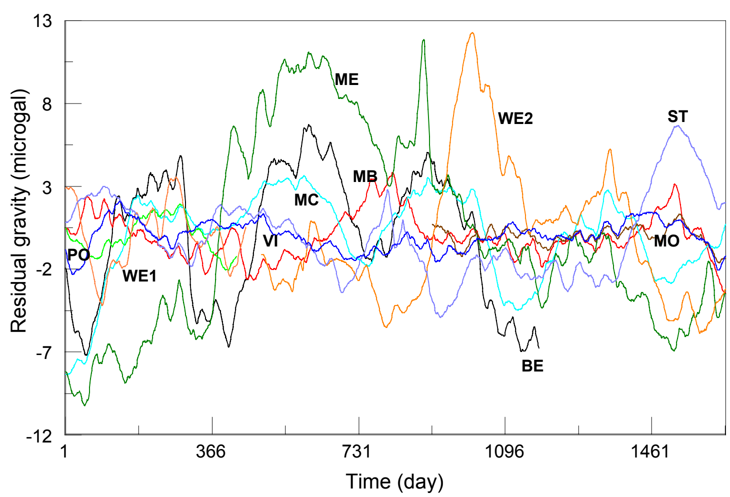

Figure 4. Individual station residuals for the 8 stations between July 1997 and December 31, 2001. Subtracted are the solid earth and ocean tides, atmospheric pressure and polar motion. Two series exist for Wettzell, and a linear drift has been subtracted from each data set.

One of the best ways of doing this is an EOF analysis, used frequently in oceanography and meteorology. At each time interval, here 15 days, the 8 stations are gridded using a minimum curvature algorithm that puts the smoothest surface through the stations. This is repeated for each 15-day sample of the field for the 4 years of the data. The EOF algorithm (see Crossley et al., 2003, 2004) finds the dominant spatial modes of the data and their time variability.

The first 4 eigenvectors are shown below in Fig 5 that together explain 95% of the variability of the data. This representation is very efficient as virtually all the data for each 15-day sample can be reconstructed from these 4 maps together with their time variation, the principal components.

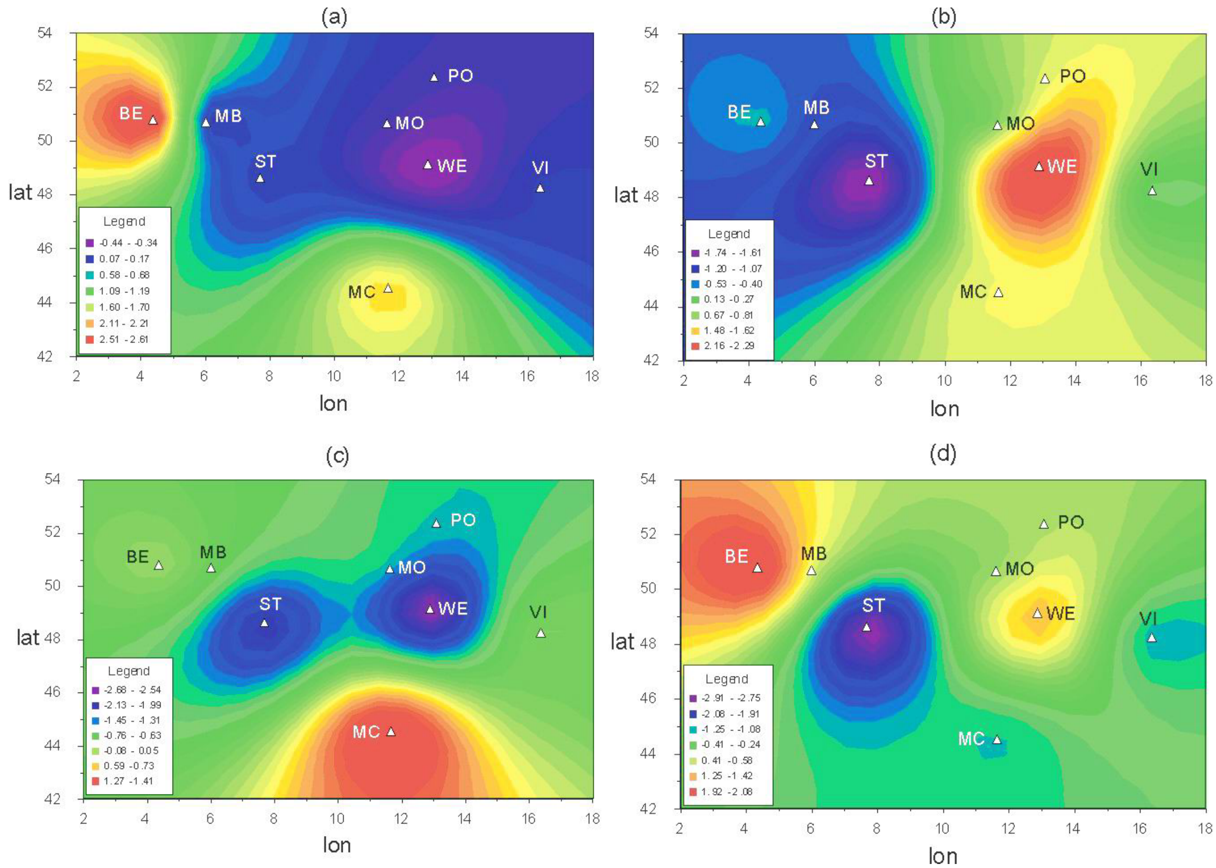

Figure 5. EOF maps of the spatial modes of the data in Fig. 4. The first four largest eigenvectors are shown: (a) first, 47% variance reduction, (b) second, 28% variance reduction, (c) third, 13% variance reduction, and (d) fourth, 7% variance reduction.

The first two principal components, representing the time variation of the data, are shown in Fig. 6. It can be readily seen that pc1 has a strong annual component, with a maximum approximately mid-winter (the series starts July 1, 1997), except for the last part of the record.

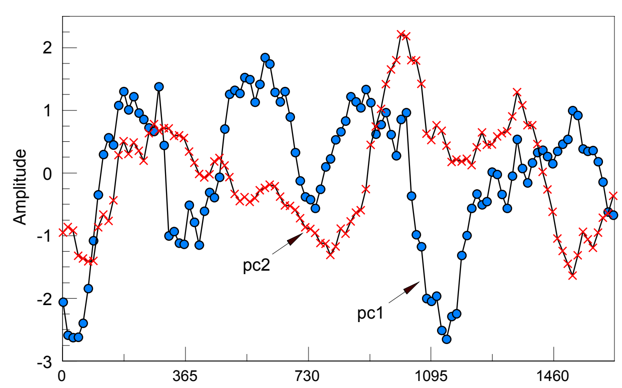

Figure 6. The first two principal components (temporal modes) of the data in Fig. 4. The first mode pc1 has a clear annual variation, but the second mode has no evident periodicity.

We now compare the gravity data with predicted hydrology, and here use the LAD model of Milly and Shmakin (2002), in which they use meteorological forcing of the climate system to predicted soil moisture and snowfall. These parameters are then used to infer the loading and deformation of the ground using simple loading models. The results for the individual stations are shown in Fig. 7, where the total equivalent gravity effect is computed. Again we see a strong annual component with amplitude of a few microgal and maxima in winter.

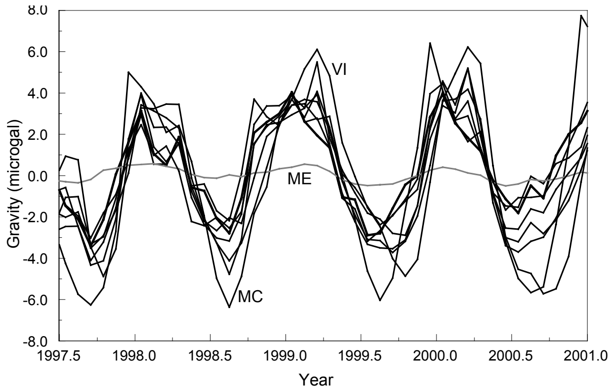

Figure 7. Combined hydrology loading and direct attraction effects from soil moisture and snow on the 9 stations. Apart from Metsahovi (ME), the hydrology effect shows an annual cycle with a constant amplitude.

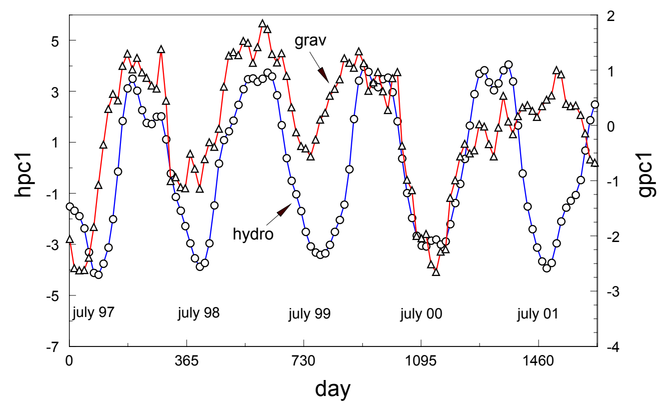

Figure 8. Comparison of the principal components of hydrology (blue curve) and gravity (red curve). The amplitudes are in arbitrary units (not µGal).

For consistency we analyze the hydrology using an EOF analysis and extract the principal component of the first eigenvector and compare it with pc1 for gravity. The comparison in Fig. 8 shows good agreement in terms of phase, and the amplitudes, when converted back to µGal, are also in agreement at about 1.5 µGal peak-to-peak.

2.2 Eighteen Month Study with GRACE Data

The question is whether these results are consistent with the GRACE data, so we perform a second experiment using data only for the 18 months we had the available GRACE data, from April 2002 to October 2003. We took 11 monthly solutions (not equally spaced) from UTCSR and computed gravity over a 0.25 ° x 0.25 ° grid zoomed over Europe using different truncation degrees (n = 5 to 50) for the spherical harmonic expansion. Geophysical corrections were made for solid earth + ocean tides, a barotropic ocean circulation model, a tabular atmosphere, and polar motion. We expect therefore that continental hydrology will be the largest remaining contribution to gravity variability on land.

We then did an EOF analysis of these 11 monthly solutions, as for gravity, over the same area as in Fig. 3 (latitude 44-52°, longitude 2-18°). The first two principal components were then extracted as before and the results shown in Fig. 9 for two truncation levels, n = 10 and n = 20. For both results there is a clear maximum in the winter of 2002-03, and a steady decrease during 2003. For Europe, similar features were seen in another recent study on GRACE data (Wahr et al. 2004). Repeating the analysis for n = 50

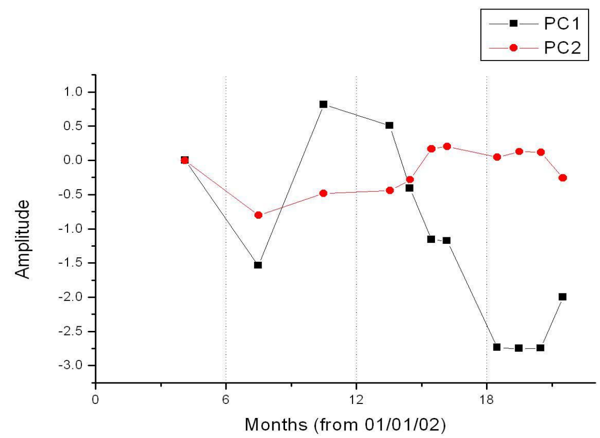

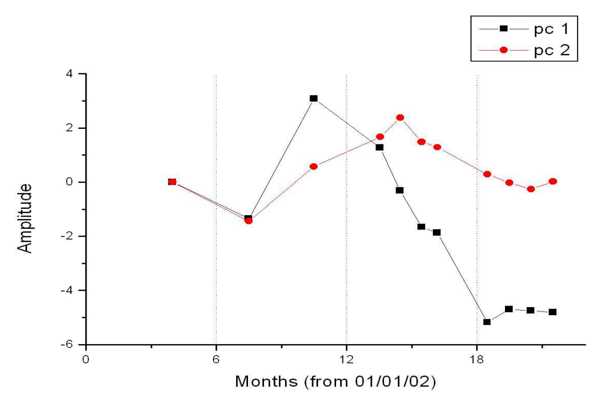

Figure 9. Principal components of the GRACE gravity fields over Europe. The first principal components gave 94% and 84% variance reduction respectively for n=10, 20.

yielded unreasonably large fluctuations in the EOF components and we believe this is because the shorter wavelength information is lacking in this version of the GRACE fields.

We then repeated the EOF decomposition applied to the GRACE field, truncated to n=20, over a larger European zone (35 to 80° latitude and –10 to 35° longitude). The results showed that the previous annual term becomes much weaker explaining only 20% of the variance. It appears reasonable that other contributions will become important over mixed land-ocean areas, such as oceans mixing with continental hydrology in Europe or the non-uniformity of hydrology at this scale.

Individual stations can be compared by interpolating the EOF decomposition to the various SG locations, and the results are shown in Fig. 10 for 4 stations. We also show the results of two hydrology models, Milly and Shmakin (2002) and Rodell et al. (2004)

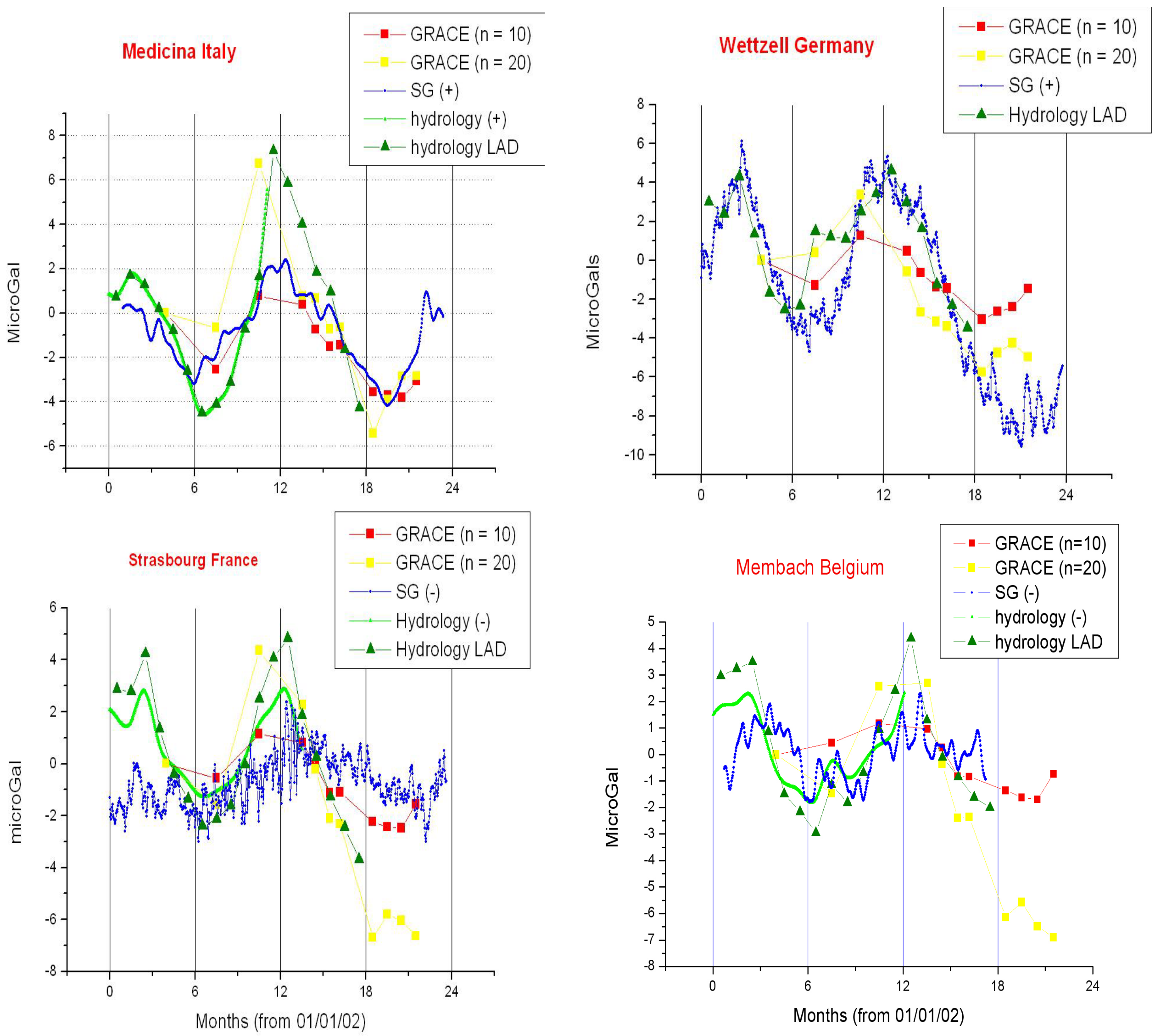

Figure 10. Comparison of SG gravity, hydrology models, and GRACE gravity. The upper two stations MC and WE show a good qualitative agreement for all variables, but the lower two stations MB and ST show poorer agreement with the SG data.

One clear reason for the difference in responses in Fig. 10 is because stations MC and WE are essentially above ground and those of ST and MB are underground installations. When a layer of water (or water saturated overburden or rock) lies above a station, one can see from Table 4 that for every cm of water, the gravity effect is 0.42 μGal, so it only takes a few cm of water above the station to counteract the effects of continental hydrology which is computed assuming the water is below the station.

For this reason it would be very useful to perform detailed terrain corrections for variable soil moisture for any station that has permeable media above it. This will be essential if the stations are to be compared to satellite data. This situation has not up to the present been a problem, but it can be important for the SG-GRACE comparison.

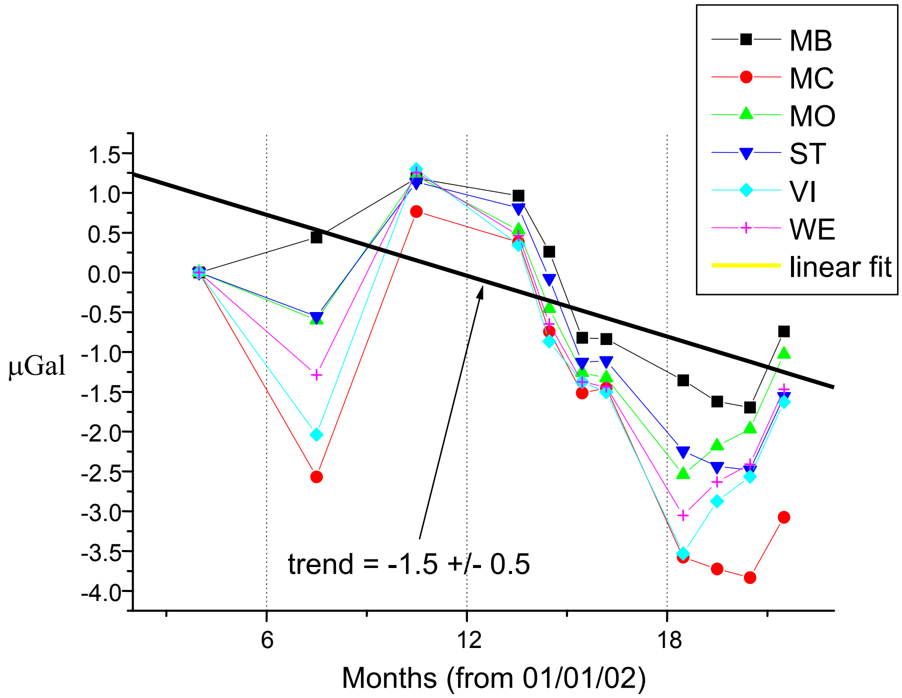

Figure 11. GRACE field samples at the SG stations showing downward trend coinciding with the summer of 2003.

Figure 11 shows all the GRACE solutions interpolated at the GGP stations for the 18-month period. As expected the coherency is high because of the large averaging footprint, but there is also some evidence for a decrease in gravity of about 1.5 μGal. To date we cannot see this in the SG records because the mean was removed from each station for the GRACE comparison. This gravity decrease in Europe is part of more global inter-annual gravity changes from GRACE, which are of hydrological origin (Andersen & Hinderer, 2004).

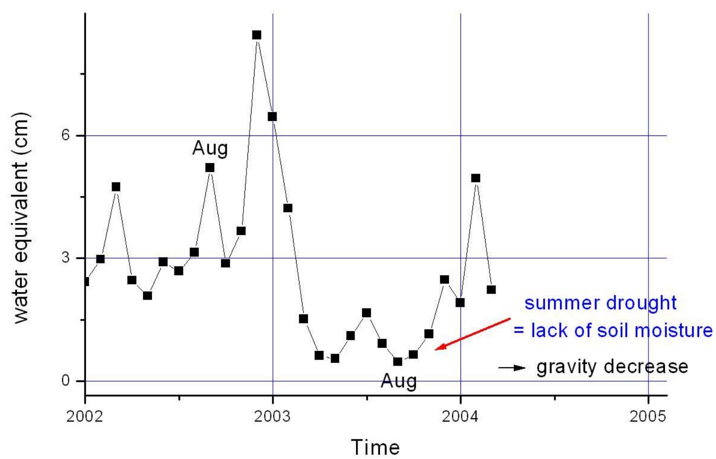

Figure 12. Average soil moisture in Europe derived from NCEP data between 2002-2004 showing the decrease in water equivalent of about 3 cm.

In future it would be interesting to check the AG measurements at the SG sites to see if indeed the overall decrease is consistent with the GRACE trend. Naturally with only 18 months of data, nothing definite can be said yet about the possible causes of such a secular change. We also note (see Fig. 12) another study showing the average soil moisture in Europe derived from NCEP using an atmospheric-derived terrestrial water storage model (Au et al. 2003). It can be seen that there is a 2 cm drop in equivalent water, which translates into about a microgal decrease in gravity. The summer of 2003 was abnormally hot and precipitation-free, so the usual annual cycle in gravity and hydrology are both affected. It will be interesting to see how the data look for 2004 when available.

3. Co-Seismic and Aseismic Deformation with Gravimeters

We here consider both co-seismic static displacements that occur soon after the onset of a normal earthquake and the separate category of slow and silent earthquakes that are long time scale aseismic events, generally of lower energy than the larger subduction earthquakes in the same location. In both cases the accelerations are at the low end of gravimetric detectability, in the range 1-2 μGal, and also distributed over areas of several 100 sq. km. They therefore present similar detection problems to the continental hydrology effects considered in the previous section.

3.1 Co-Seismic (or Static) Deformation.

Turning first to co-seismic deformation, this has long been treated both using the theory of earthquake faulting (e.g. Jiao et al., 1995) and within the context of normal mode theory. Ekstrom (1995) presented a study of the static displacement field computed from the sum of normal modes from the deep Bolivia event in 1994. The idea is to compute the static displacement as the sum of all the Earth's normal modes, including in principle all the modes hidden in the liquid core and solid inner core (though these are rarely considered for surface displacement). The excitation requires knowledge of the source mechanism and an appropriate catalogue of all the mode eigenfunctions. Ekstrom found that the final displacement of –7mm was achieved over a period of 6-7 min after the earthquake rupture, but this was within a few 100 km of the event. Displacements of greater than 1 mm were found out to about 2000 km. In terms of gravity, Table 4 shows that the gravity change would be only about 1 μGal and this would be possible to identify only with an SG close to the event and within a definite time window. GPS measurements were not available for comparison, but a few mm is a challenge in the vertical.

Coseismic deformation was observed gravimetrically by Goodkind (1995) in records of SG observations in Alaska. Figure 13 shows two coseismic events in 1993 that are clearly related both to jumps in cumulative seismic energy release and to gravity offsets of 1-2 μGal. Although the correlation between the seismology and the gravity is convincing, in general it is very difficult to be sure of gravity changes at the few microgal from a single instrument. For this reason an array of SGs is necessary to be certain of identifying coseismic deformation. Note the beginning of the gravity changes appear to precede the seismic events.

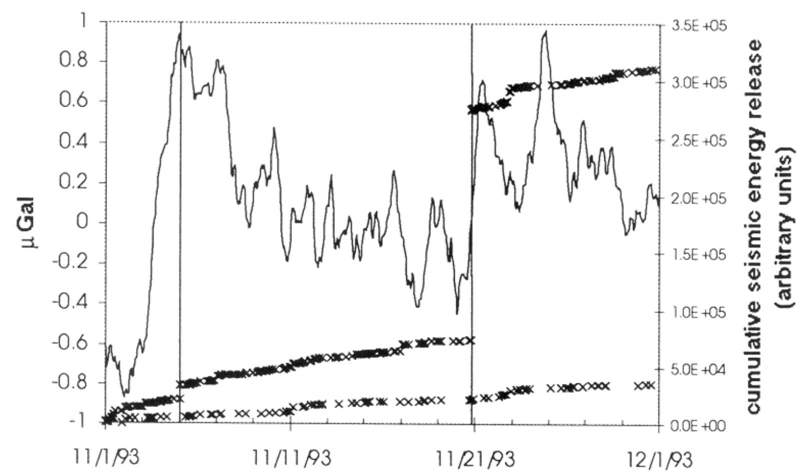

Figure 13. Recording of two earthquakes (vertical lines) in Alaska (4.1 mb and 5.3 mb respectively) recorded by an SG at Fairbanks in 1993. The continuous curve is the gravity residual. The x's are cumulative seismic energy, the upper curve is for all events around the station and the lower is for events only in central Alaska, from Goodkind (1995).

Recently Imanishi et al. (2004) have demonstrated that co-seismic displacement of a few mm could be detected from the Mw 8.0 Tokachi-oki earthquake on Sept. 2003 off the coast of Japan. They used the 3 Japanese SGs in Esashi, Matsushiro and Kyoto (Fig. 14). The epicenter is almost in line with the 3 SGs and it is an ideal event for studying co-seismic deformation. The data were carefully processed to remove the effects of hydrology before the offsets due to the earthquake were estimated. The results are shown in Fig. 15 where the large surface waves have been windowed out of the residual gravity (tides, and air pressure removed). It can be seen that the offsets decease away from the epicenter, as expected, and also are very small (at the limit of detectability). One advantage of looking for such effects in gravity is that the static displacement can be well modeled using seismic source theory, and the time of the offset is well constrained. In this example, the estimated offsets are consistent with the theoretical values obtained using the theory of Okubo (1993) and Sun and Okubo (1998).

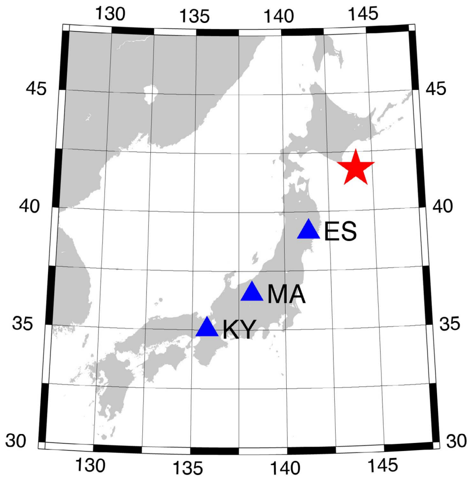

Figure 14. SGs in Japan, with the star denoting the epicenter, from Imanishi et al. (2004).

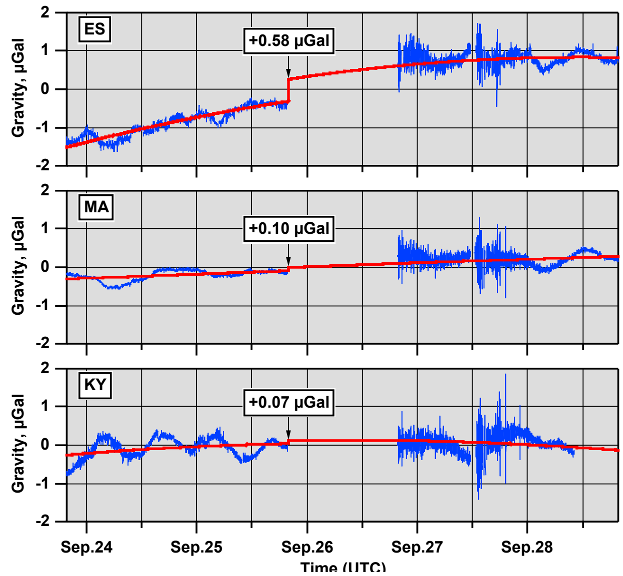

Figure 15. Static displacements recorded at SG stations, from Imanishi et al. (2004).

Table 5. Calculated and Observed Static Deformation

		Calculated Acceleration (μGal)			Observed
Station	□ (deg)	Redistribution	Displacement	Total	(μGal)
Esashi	3.4	+0.134	+0.485	+0.619	+0.58 unequivocal
Matsushiro	6.9	+0.171	–0.048	+0.123	+0.10 less certain
Kyoto	9.4	–0.239	+0.296	+0.057	+0.07 marginal

3.2 Slow and Silent Earthquakes.

Beroza and Jordan (1990) brought widespread attention to the existence of this class of earthquake rupture through their study of normal modes that could be detected on seismograms but which had no apparent seismic source event. We now recognize that there is a continuous spectrum of free oscillations, constantly excited by the broadband energy of both atmospheric and oceanic sources (Rhie and Romanowicz, 2004), but presumably the free oscillations detected by Beroza and Jordan are still distinct from this background.

Recently there has been considerable interest in the observation of silent slip events associated with the subduction of oceanic plates. Perhaps the most studied area is the Cascadia subduction zone in the Eastern Pacific ocean off the coast of Vancouver Island

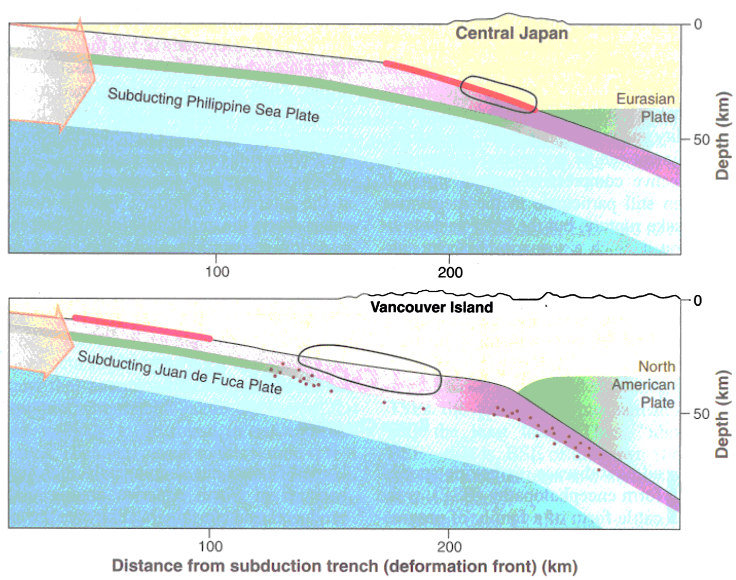

Figure 16. Similarities and differences in the subduction zones off Nankai (Japan) and Vancouver Island (Canada). The red boundary is where large earthquakes occur and the silent slip occurs in the elongated regions, from Rhie and Romanowicz (2004).

(Hirn and Laigle, 2004), but other notable examples off the coasts of Japan and the Phillipines are discussed by Kawasaki (2004). Fig. 16 shows a comparison of the Nankai subduction zone with the Cascadia subduction zone. Silent earthquakes are not themselves dangerous, but they do offer unique insight into the mechanics of subduction and may lead to a predictive mechanism for the large thrust events that could cause damage in both sides of the Pacific.

As discussed by Dragert et al. (2001), a silent slip event under Vancouver Island was detected by GPS measurements. Subsequently, Rogers and Dragert (2003) discussed the repetitive nature of the slip events following a regular pattern and called the phenomena episodic tremor and slip. Figure 17 shows the topology of a single event, as detected by GPS. Note the event is opposite in direction to the main NE thrust of the Juan de Fuca plate. Fig 18 is for the episodic slip.

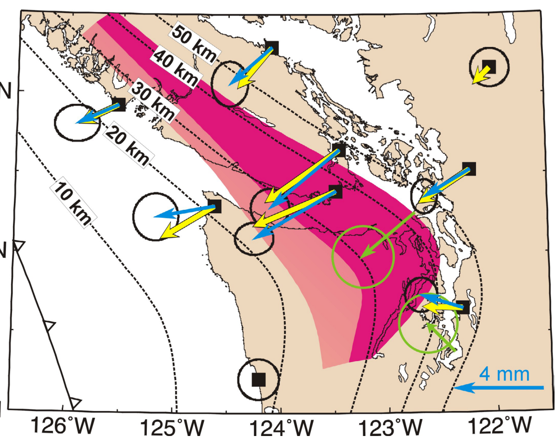

Figure 17. Slip event during 1999 transient event. Blue arrows with error ellipses are the GPS measurements and yellow arrows are from the model of a simple stick-slip mechanism that evolves from SE to NW.

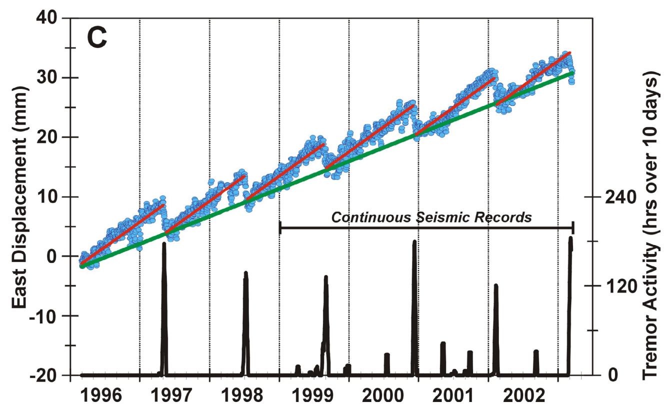

Figure 18. Periodic slip events detected by GPS as displacements and seen as enhanced seismic activity in the vertical spikes.

Gravity measurements of this slip have been recorded by an absolute gravimeter at Ucluelet, a town on the Western side of Vancouver Island (Fig. 19). It can be seen, as predicted in Table 1, that the AG accuracy of about 2 μGal is not quite enough to clearly follow the expected gravity changes due to the slip events, but there is a clear indication that gravity is consistent with the model. The use of 1-3 SGs on Vancouver Island would immeasurably help to identify the slip events to a fraction of a μGal.

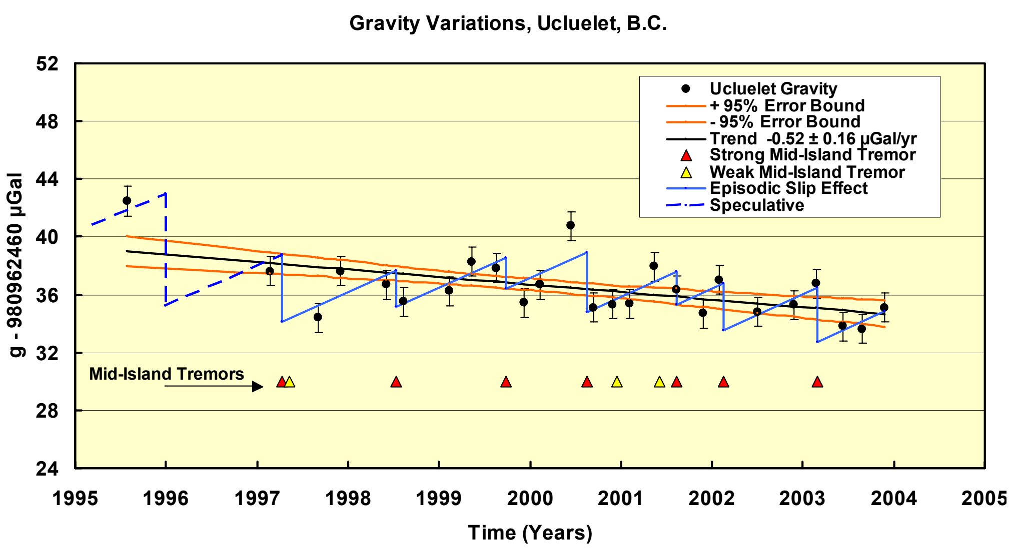

Figure 19. Episodic gravity variations - model and AG observations (Lambert, 2004)

4. Gravimetry on Volcanoes

We here give a sampling of some studies that have been done using gravimetry in a volcanic setting. There are many more papers that should be included if we were to attempt a more comprehensive survey of the field. Most studies prior to 1995 used LaCoste & Romberg (LCR) D and G relative meters, which have an accuracy of 3-5 μGal in the best-case scenario, but since the mid 1990's a new instrument, the Scintrex GC-3M relative meter, has demonstrated several advantages (and comparable accuracy to the LCR) for measurements in rugged terrain (Budetta and Carbone, 1997).

We note here that variations of 1–100 μGal are typically to be expected from changes in the subsurface magma distribution over periods of months to years (excluding eruptive events). We refer the reader to the review of Rymer and Locke (1993) who give some of the basic gravity equations and discuss the interpretation of measurements of simultaneous gravity and height variations. Fig. 20, from their paper, summarizes the 4 zones that divide the plot of Δg vs. Δh (note that the BA line value, as given in Table 4, is the normal expectation from gravity surveys):

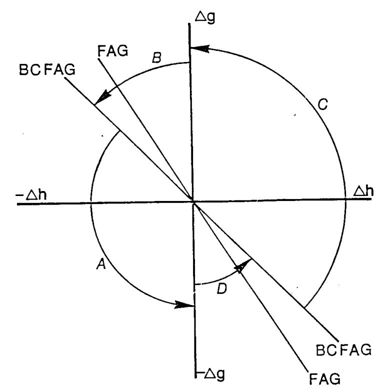

Figure 20. Regions of Δg vs. Δh changes for volcanoes, from Rymer and Locke (1993).

- Zone A is where deflation (surface lowering) is accompanied by a smaller Δg increase than the FA or BCFA prediction (see Table 4), caused e.g. by loss of magma but no collapse,
- Zone B where deflation with Δg higher than predicted, caused e.g. by replacement of gas or voids by magma injection,
- Zone C where inflation (upward doming) is accompanied by a smaller Δg than predicted, caused by e.g. replacement of voids by magma, and
- Zone D where inflation is accompanied by a greater gravity decrease than expected, caused e.g. by increase gas pressure forcing magma to lower depths.

As in all gravity studies, multiple modeling possibilities have to be considered, and special attention has to be paid to the removal of the effects of fluid and water, before interpreting the Δg and Δh changes. We note that other volcanoes that have been studied using gravity are Galeras, Columbia (Jentzsch et al., 2000) and Usu, Hokkaido, Japan (Jousset et al., 2003).

4.1 Surveys Using One Type of Instrument.

As one of the earlier studies, Lagios (1991) reported on gravity observations over the Thera Volcano on the island of Santorini, Greece. Measurements were made annually between 1984 and 1991 at 25 stations over an area of 15 x 20 km using 3 LCR instruments. Particular attention was paid to maintain the height consistency of station visits to within 5 mm (1.5 μGal) and the pressure was measured to 0.01 mbar (0.003 μGal). Three stations showed an overall increase of > 20 μGal, and overall the island is separated into regions of uplift and subsidence (± 5 μGal/yr). No significant density changes could be attributed to magmatic sources, and the systematic trends suggested a possible tectonic source. A GPS array was planned for 1993, and a report of measurements between 1993 and 200 was given by Stiros (2000), but no further gravimetric information has been found for this site.

Jahr et al. (1995) reported gravity measurements on Mayon Volcano, Luzon, in the Phillipines. The survey, using 10 stations, was done in 1992, and again 5 months later in 1993, using 3 LCR gravimeters. Results showed station differences varied from -60 to +80 μGal along the profile, but no modeling was done. Jentzsch et al. (1995) discussed the possibility that tidal stresses could be a factor in triggering eruptions.

Gerstenecker and Suyanto (1998) reported a campaign of gravity observations on Mt. Merapi, Indonesia covering the period 1996-1997. Previous work had set up a large network of more than 500 stations over an area of 2000 sq km that had routinely been surveyed between 1970 and 1996. Previous models had suggested that there may be a 50μGal anomaly associated with the magma chamber, but it was too small to be seen in their study. Gerstenecker et al. (2000) later reported on a one-year study between 1997 and 1998, in which elevation changes of 10-15 cm at the summit were found from GPS measurements. They found a general gravity increase after the last eruption (July 98), but its amplitude is impossible to read from the figure in the paper. It was noted that the gravity increase was not correlated with an elevation change.

El Wahabi et al. (1997), carried out a rather different kind of study on Mt. Etna, Sicily, between 1991 and 1995. LCR gravity measurements were sampled every minute at 2 stations, separated by about 20 km. The data was subject to standard tidal analysis and residual gravity variations of + 500 μGal and ± 250 μGal were apparent for the 2 stations. The detection threshold for events was estimated for the two instruments at 9-15 μGal. There were some unanswered questions about instrumental effects and further planning was not stated.

4.2 Surveys Using Multiple Instrument Types

Budetta and Carpone (1997) were one of the first groups to use the Scintrex CG-3M gravimeter for volcanic studies, and they demonstrated that the accuracy of the residuals at 3-4 μGal were similar to the best that had been obtained from the LCR instruments. Careful attention to procedure reduced the drift estimates to 20 μGal d^{-1} and calibration factors were determined to 30 ppm. In a further study, Carbone et al. (2003a) used both continuous and discrete surveys (Scintrex and LCR gravimeters respectively) to increase the reliability of measurements to an accuracy of 10 μGal between the different instruments.

On Merapi volcano, Indonesia, Jousset et al. (2000) reported the use of the Scintrex CG3 gravimeter to measure gravity changes between 1993 and 1995, with GPS for locations. The GPS indicated elevation changes of only 5 cm (15 μGal), but larger gravity changes of +400 to –270 μGal we seen that could be associated with growth of the dome and increase of mass under part of the summit. To assist in monitoring instrument drift, a semi-permanent station was set up 4 km from the summit with a continuous gravimeter (presumably LCR type). Residual gravity was correlated with seismic and volcanic activity (through processes such as crystallization of the magma), but the relatively large drift of the LCR instrument reduces confidence in the final determination.

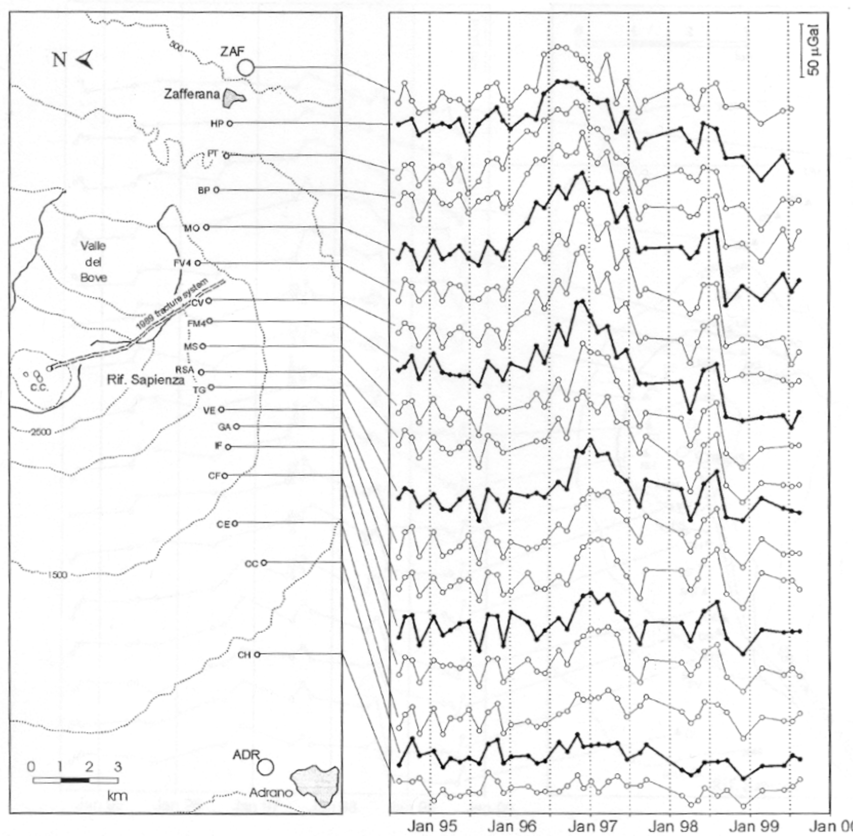

Figure 21. A gravity profile E-W on the south flank of Mt. Etna for August 1994 – August 1999, corrected for water table fluctuations. Stations ZAF (Zafferana) and ADR (Adrano) are reference stations. Note the gravity increase of at least 50 μGal during 1996 and the decrease thereafter, from Carbone et al. (2003a).

In two more recent papers on Mt. Etna, Budetta et al. (1999) and Carbone et al. (2003b) report on the extension of the gravity network using more stations and better controls and they confirmed the better reliability of the Scintrex CG-3M gravimeter compared to previous LCR results. Fig. 21 from Carbone et al. (2003a) shows an EW profile of about 24 km in which gravity fluctuations of > 100 µGal occur over the two year period, and individual errors are assessed at 7 µGal. In this paper, the important effect of water table fluctuations is also included in the assessment of the magmatic processes. In the second paper, the authors discuss in detail the interpretation of the GPS and gravimetric data in terms of magmatic activity and water table fluctuations over the whole 5-year period.

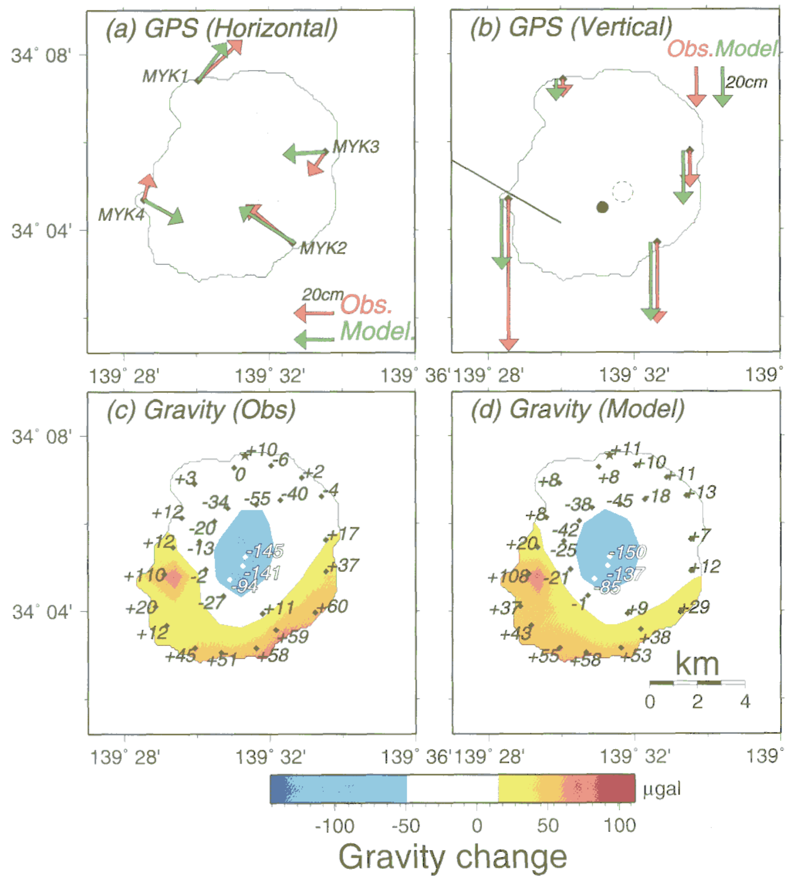

Figure 22. GPS and gravity variations just prior to the collapse of the caldera, from Furuya et al. (2003).

Finally, we conclude with the paper of Furuya et al. (2003) on gravity changes at Miyakejima Volcano, Japan. The authors use a different combination of instruments, an absolute gravimeter (FG5) as the base station, and 2-3 LCR gravimeters to do the roving surveys. An accuracy of 2-3 µGal is estimated for the AG at the reference site, and the nominal accuracy of the LCRs is 10 µGal. This is the first use of an AG to detect absolute gravity changes. Other instrumentation on the volcano consisted of 4 GPS stations and 5 tiltmeters. A typical result is shown in Fig 22 for the GPS and gravity changes over a 2-year period just prior to the collapse of the summit of the volcano in 2000. Again, the combined instrumentation allows the authors greater possibilities for modeling the density changes independently of the surface deformation.

4.3 Prospects for Using SG Arrays

Given the earlier examples, it would be easy to be skeptical about the possibility of closely monitoring gravity changes on volcanoes. Fundamental logistic difficulties, and the scarcity of suitable instrumentation were the most common early problems. The more recent papers on the use of multiple gravimetry, however, show that great progress has been made in refining the observations to accuracies of 10 µGal or perhaps even less, and this is enough for some detailed modeling to be done.

Nevertheless, two limitations can be seen in the use of the LCR and Scintrex instruments: one is the problem of large instrument drift and the other is that of unstable calibration. There is a large amount of evidence to suggest that the SG can all but eliminate these two problems because its annual drift is essentially within the accuracy of the Scintrex instrument (few µGal yr^{-1}) and its calibration is remarkably constant. If one were to use at least one SG (preferably a group of 3, if possible) as a reference station and 2-3 Scintrex instruments doing repeated surveys at monthly intervals, it should be possible to cover areas of several 100 sq km with relative accuracies of perhaps 3 µGal, which is better by factors of 2-3 than present surveys. This improvement may be significant if one is looking for subtle gravity precursors to a large eruption in a potentially life-threatening situation. An appropriate GPS array is of course necessary to account for possible elevation changes at the gravity stations; this in itself is a non-trivial task. For long term monitoring, an SG needs to be visited every 6 months or so by an absolute gravimeter to check calibration (not usually changing) and drift.

A campaign such as that envisaged above, involving 3 types of gravimeters, would be demanding in equipment and resources and require extensive cooperation between scientific groups over several years. But given the success of the more recent studies (cited above) in which multi-instruments have already been used, it is clearly now possible to employ the field transportable SG on volcanoes. The caveat is that the instrument should remain stationary for several months or longer, and that sufficient logistic support should be available in case of equipment failure. The latter requirement favors locations such as Mt. Etna and some of the Japanese volcanoes that are relatively near to modern facilities and resources.

5. Conclusions

We have demonstrated that widely spaced SGs in Europe do respond to common signals of about the right amplitude (1-3 μGal) and phase to be associated with continental hydrology (as predicted by recent models). Further, both signals are also consistent in amplitude and phase with our processing of the first 18 months of GRACE data and we are encouraged to believe there is a valid connection between the data sets. At the present time the best agreement would seem to be with GRACE models that are truncated at degree $n = 20$. The question of the correction of SG residuals due to local hydrology, e.g. soil moisture, especially in a surface layer above a gravimeter (as opposed to below it), remains a difficulty that can only be addressed with detailed local models.

We have extended our discussion to coseismic deformation and deformation associated with silent slip events in subduction zones. The gravity effect of both these is at the few μGal level and probably best detected using an array of 3 or more SGs. The first results from Japan (Imanishi et al, 2004) on co-seismic displacement are quite encouraging at the 1 μGal level and consistent with theoretical expectations for a large earthquake. It would appear such levels are below that detectable with an AG.

Ground monitoring of silent slip events, such as has been described for the Cascadia subduction zone would require 3 or more SGs, together with an AG (that by itself cannot resolve the slip unambiguously). When combined with existing GPS networks, one may hope to learn more about the type of deformation involved in a silent slip event, especially in a situation where there is repeated slip at regular intervals. It would also be particularly interesting to identify any pre-cursor signals that might appear before a major thrust event.

As far as volcanoes are concerned, the gravity effects are much larger, up to 100 μGal or more. The requirement for dense station coverage would suggest the use of SGs as primarily base stations. The bulk of the field observations are probably best left to the Scintrex type field gravimeters due to their ease of use. As has already been demonstrated, the combination of different instruments makes for a much more reliable and accurate observational program that should give insight to the mass motions that occur beneath active volcanoes.

Acknowledgments

We wish to thank the GGP station operators, especially those who provided data directly: H. Wilmes (WE), H. Virtanen (ME), M. van Camp (MB), B. Meurers (VI), B. Richter (MC), and C. Kroner (MO). We also thank P. Milly and M. Rodell for providing updated hydrology models. Y. Imanishi and T. Lambert provided results ahead of publication, and J.-P. Boy and F. Lemoine (NASA) assisted in the data processing.

References

Andersen, O., and Hinderer, J., 2004. Global inter-annual gravity changes from GRACE: early results, Geophys. Res. Lett., in press.

Au, A.Y., B.F. Chao, M. Rodell and T.J. Johnson, 2003, Global Soil Moisture Field and the Effects on the Earth's Gravity. Paper presented at Workshop on Hydrology from Space, http://gos.legos.free.fr/, Toulouse, France, 29 Sept - 1 Oct.

Beroza, G. C. and T. H. Jordan, 1990. Searching for slow and silent earthquakes using free oscillations, *J. Geophys. Res.* **95**, 2485-2510.
Budetta, G., and D. Carbone, 1997. Potential application of the Scintrex CG-3M gravimeter for monitoring volcanic activity; results of field trials on Mt. Etna, Sicily, *Journal of Volcanology and Geothermal Research*, **76** (3-4), 199-214.
Budetta, G., D. Carbone, and F. Greco, 1999. Subsurface mass redistributions at Mount Etna (Italy) during the 1995-1996 explosive activity detected by microgravimetry studies, *Geophys. J. Int*., **138**, 77-88.
Carbone, D., G. Budetta, and F. Greco, 2003a. Possible mechanisms of magma redistribution under Mt. Etna during the 1994-1999 period detected through microgravimetry measurements, *Geophs. J. Int*., **153**, 187-200.
Carbone, D., F. Greco, and G. Budetta, 2003b. Combined discrete and continuous gravity observations at Mount Etna, *J. Volcan. Geotherm. Res*., **123** (1-2), 123-135.
Crossley, D. J., J. Hinderer, G. Casula, O. Francis, H. -T. Hsu, Y. Imanishi, B. Meurers, J. Neumeyer, B. Richter, K. Shibuya, T. Sato and T. van Dam, 1999. Network of superconducting gravimeters benefits several disciplines, *EOS*, **80**, pp. 121-126.
Crossley, D., J. Hinderer, N. Florsch and M. Llubes, 2003. The potential of ground gravity measurements to validate GRACE data, *Advances in Geosciences* **1**, 65-71.
Crossley, D., J. Hinderer, and J. -P. Boy, 2004. Regional gravity variations in Europe from superconducting gravimeters, *J. Geodynamics*, 38, 325-342.
Dragert, H. K. Wang, and T. S. James, 2001. A silent slip event on the deeper Cascadia subduction interface, *Science*, **295**, 1525-1528.
Ekstrom, G., 1995. Calculation of static deformation following the Bolivian earthquake by summation of the Earth's normal modes, *Geophys. Res. Lett.*, **22** (16), 2289-2292.
El Wahabi, B. Ducarme, M. van Ruymbeke, N. d'Oreye, and A. Somerhausen, 2000. Continuous gravity observations at Mount Etna (Sicily) and correlations between temperature and gravimetric records in: *Proceedings of the workshop on short term thermal and hydrological signatures related to tectonic activities,* **14**, 105-119, Cahiers du Centre Européen de Géodynamique et de Séismologie, Luxembourg,
Furuya, M., S. Okubo, W. Sun, Y. Tanake, J. Oikawa, and H. Watanabe, 2003. Spatiotemporal gravity changes at Miyakejima Volcano, Japan: caldera collapse, explosive eruptions, and magma movement, *J. Geophys. Res.,* **108**, B4, 2219.
Gerstenecker, C. and I. Suyanto, 2000 Gravity mapping of Merapi and Merbabu, Indonesia, in: *Proceedings of the Workshop: High precision gravity measurements with application to geodynamics and second GGP Workshop*, **17**, 193-200, Cahiers du Centre Européen de Géodynamique et de Séismologie ECGS, Luxembourg.
Gerstenecker, C., G. Jentzsch, G. Lamfer, B. Snitil, I. Suyanto, and A. Weise, 2000. Repetition network and digital elevation models at Merapi, Indonesia, in: *Proceedings of the Workshop: High precision gravity measurements with application to geodynamics and second GGP Workshop*, **17**, 210-205, Cahiers du Centre Européen de Géodynamique et de Séismologie ECGS, Luxembourg.
Goodkind, J. M., 1995. Gravity peaks at the time of earthquakes in central Alaska, in *Proceedings of Second Workshop: Non-tidal gravity changes Intercomparison between absolute and superconducting gravimeters,* **11**, 91-96, Cahiers du Centre Européen de Géodynamique et de Séismologie, Luxembourg.
Hinderer, J., and Crossley, D., 2004. Scientific achievements from the first phase (1997-2003) of the Global Geodynamics Project using a worldwide network of superconducting gravimeters, J. Geodynamics, **38**, 237-262.
Hirn, A. and M. Laigle, 2004. Silent heralds of megathrust earthquakes? *Science*, **305**, 1917-18.
Imanishi, Y., T. Sato, T. Higashi, W. Sun and S. Okubo, 2004. A network of superconducting gravimeters detects submicrogal coseismic gravity changes, *Science*, **306**, 476-478.
Jahr, T., G. Jentzsch, and E. Diao, 1995. Microgravity measurements at Mayon Volcano, Luzon, Philippines in: *Proceeding of the Workshop: New challenges for geodesy in volcanoes monitoring*, **8**, 307-317, Cahiers du Centre Européen de Géodynamique et de Séismologie, Luxembourg,
Jentzsch, G., O. Haase, C. Kroner, U. Winter, and R. S. Punongbayan, 1997. Tidal triggering at Mayon Volcano?, in: *Proceedings of the workshop on Short term thermal and hydrological signatures related to tectonic activities*, **14,** 95-104, Cahiers du Centre Europeen de Geodynamique et de Seismologie ECGS
Jentzsch, G., M. Calvache, A. Bermudez, M. Ordonez, A. Weise, and G. Moncayo, 2000.Microgravity and GPS at Galeras Volcano/Colombia; the new network and first results in: *Decade volcanoes under investigation*, **2000** (4), 49-52, Deutsche Geophysikalische Gesellschaft, Munster.
Jiao, W., T. Wallace, and S. Beck, 1995. Evidence for static displacements from the June 9, 1994 deep Bolivian earthquake, *Geophys. Res. Lett.,* **22** (16), 2285-2288.

Jousset, P., Dwipa, S., Beauducel, F, Duquesnoy, T. and Diament, M., (2000). Temporal gravity at Merapi during the 1993-1995 crisis; an insight into the dynamical behavior of volcanoes, *Journal of Volcanology and Geothermal Research*, July 2000, **100 (**1-4), 289-320.

Jousset, P. H. Mori, and H. Okada, 2003. Elastic models for the magma intrusion associated with the 2000 eruption of Usu Volcano, Hokkaido, Japan, *Journal of Volcanology and Geothermal Research*, **125**, (1-2), 81-106.

Kawasaki, I., 2004. Silent earthquakes occurring in a stable-unstable transition zone and implications for earthquake prediction, *Earth, Planets, Space*, **56**, 813-821.

Klopping, F.J., Peter, G., Berstis, K.A., Carter, W.E., Goodkind, J.M. and Richter, B.D., 1995, Analysis of two 525 day long data sets obtained with two side-by-side, simultaneously recording superconducting gravimeters at Richmond, Florida, U.S.A., in *Proceedings of Second Workshop: Non-tidal gravity changes Intercomparison between absolute and superconducting gravimeters,* **11**, 57-69, Cahiers du Centre Européen de Géodynamique et de Séismologie, Luxembourg.

Kroner, C. T. Jahr, and G. Jentzsch. 2001. Comparison of Data Sets Recorded with the Dual Sphere Superconducting Gravimeter CD 034 at the Geodynamic Observatory, Moxa. *J. Geod. Soc Japan*, **47 (1)**, 398-403.

Lagios, E., 1995. High precision study of gravity variations over the Thera volcano, Greece, in: *Proceedings of the Workshop: New Challenges for Geodesy in Volcano Monitoring*, **8**, 293-305, Cahiers du Centre Européen de Géodynamique et de Séismologie, Luxembourg.

Merriam, J. B., 1993. Calibration, phase stability, and a search for non-linear effects in data from the superconducting gravimeter at Cantley, Quebec, in *Proceedings of the 12th International Symposium on Earth Tides, Beijing, China,* **12**, ed H. -T. Hsu, Science Press, Beijing.

Milly and Shmakin, 2002. Global modeling of land water and energy balances, part I: the land dynamics (LaD) model, *J. Hydrometeorology*, **3**, 283-299.

Okubo, S., 1993. Potential and gravity changes due to shear and tensile faults in a half-space, *J. Geophys. Res*. **97**, 7137-7144.

Rhie, J. and B. Romanowicz, 2004. Excitation of Earth's continuous free oscillations by atmosphere-ocean-seafloor coupling, *Nature*, **431**, 552-555.

Rodell, M., P. R. Houser, U. Jambor, J. Gottschalck, K. Mitchell, C. -J. Meng, K. Arsenault, B. Cosgrove, J. Radakovich, M. Bosilovich, J. K. Entin, J. P. Walker, D. Lohmann, and D. Toll (2004), The Global Land Data Assimilation System, *Bull. Amer. Meteor. Soc*., **85** (3), 381–394.

Rogers, G. and H. Dragert, 2003. Episodic Tremor and Slip on the Cascadia Subduction Zone: The Chatter of Silent Slip, Science, **300** (5627), 0036-8075.

Rymer, H. and C. Locke, 1995. Microgravity and ground deformation precursors to eruption: a review, in: *Proceedings of the Workshop: New Challenges for Geodesy in Volcano Monitoring*, **8**, 21-39, Cahiers du Centre Européen de Géodynamique et de Séismologie, Luxembourg.

Stiros, S. C., 2000. Geodetic monitoring of the Santorini (Thera) Volcano*, Survey Review*, **37**, (287), 84-88.

Sun, W. and S. Okubo, 1998, Surface potential and gravity changes due to internal dislocations in a spherical Earth; II, Application to a finite fault, *Geophys. J. Int*., **132**, 79-88.

Wahr, J, S. Swenson, V Zlotnicki and I. Velicogna (2004), Time-variable gravity from GRACE: First results, Geophys. Res. Lett., Vol. 31, L11501 doi: 10.1029/2004GL019779.